A Receiver Phase and Group Delay Calibration System for Use in Very Long Baseline Interferometry

A.E.E. Rogers

Haystack Observatory Technical Note 1975-6

Introduction

Very-long-baseline interferometer systems used for Geodetic applications have to be either extremely phase and delay stable or be accurately calibrated. This report describes a phase and group delay calibration system with millimeter level precision. The calibrator consists of two basic subsystems. The first is a tunnel-diode pulse generator which has already been described in Haystack Technical Note 1975-1 and the second is a cable phase delay measurement subsystem. Also included in the calibration system is a broadband noise source for radiometer noise temperature calibration.

General System Description

The system utilizes the 5 MHz output from the frequency standard to produce short duration (<50 picosecond) calibration pulses at a 1 MHz rate. These pulses are injected into the receiver through an input coupler and are detected by the VLBI processing system. The calibration pulses are generated at a precisely known epoch within the one microsecond ambiguity. A component of the 5 MHz signal used to generate the calibration pulses is returned along the same cable and phase compared with the transmitted signal in order to precisely determine the phase delay (with 200 nanosecond ambiguity) in the cable driving the calibration pulse generator. The system block diagram is shown in Figure 1. The reflected 5 MHz signal is modulated in order that it may be distinguished from other intermediate reflections. In addition a component of the calibration pulse itself is returned along the cable and can be viewed on an oscilloscope to resolve the 200 nanosecond ambiguity present in the cable measurement subsystem.

Phase Calibration pulse generator

1) General Description

The phase calibrator consists of a tunnel-diode pulse generator driven by a 5 MHz square wave. The pulses (both positive and negative) emerge from the tunnel diode and are gated with a diode attenuator so that only one positive pulse per microsecond appears at the output. The block diagram of the calibrator is shown in Figure 2.

2) Pulse Duration

The tunnel-diode switching time t (at constant current) is given approximately by equation (1) for constant a current drive.

$$t \simeq \left(\frac{V_{FP} - V_P}{I_p - I_V} \right) C_V \qquad (1)$$

Where V_{FP} = Forward voltage ≃ 575 mv

V_P = Peak point voltage ≃ 90 mv

I_P = Peak point current ≃ 10 ma*

I_V = Valley point current ≃ 1 ma

C_V = Valley point terminal capacitance ≃ 1 pf

Thus t ≃ 50 picoseconds.

The condition of constant current is not well maintained as the driving impedance is close to 50Ω so that the load line intersection point is somewhat below V_{FP}. The effect is to reduce the pulse voltage without having much effect on the switching time. A sketch of the diode voltage-current characteristic is shown in Figure 3.

3) Output Power

The output temperature (averaged over several MHz) is approximately

* Increased to 16 ma. in later units

$$\left[\frac{2(V_L - V_P)^2}{R_L}\right]\left(\frac{1}{\left(\frac{\omega^2 t^2}{12}\right)+1}\right)\left(\frac{1}{T}\right)\left(\frac{1}{K\omega^2}\right) \simeq 5 \times 10^4 °K \quad \text{(at 10 GHz)} \qquad (2)$$

where $\omega/2\pi$ = Center Frequency

T = Pulse Repetition Period

R_L = Load Resistance Seen by Diode

K = Boltzmann Constant

V_L = Load line intersection voltage

4) Sensitivity to Temperature

There are a number of different effects which make the calibrator temperature sensitive.

a) Differential drifts in clipping levels

$$\Delta t \simeq \left(\frac{T}{2\pi}\right)\left(\frac{\Delta V}{V}\right) \qquad (3)$$

where T = period of input 200 nanosec, and

$\left(\frac{\Delta V}{V}\right)$ = fractional differential voltage drift

so that $\Delta T \simeq$ 300 ps/percentage differential voltage drift

b) Variations in V_P - the voltage at which the tunnel diode changes current state. From this cause

$$\Delta t \simeq \Delta T \left(\frac{\Delta V_P}{V_m}\right) \qquad (4)$$

where ΔT = risetime of driving waveform (approx. 2 nanosec.)

$$\frac{\Delta V_P}{V_m} \simeq \text{fractional drift in } V_P$$

thus $\Delta t \simeq$ 20 ps/percentage drift

c) Variations in the delay through the filter and wide-band amplifier and diode attenuator.

5) Measurements of Calibrator Performance

a) Output power within a 360-kHz band was measured by comparing output with that of a noise tube. The level was found to be 60°K at 7850 MHz when coupled into the receiver through a 30 db coupler.

b) The stability of the calibrator was measured by observing the phase of the frequency rails from the calibrator (mixed down to 1 KHz) in the receiver video output. The overall sensitivity of the phase calibrator to temperature changes was measured by cycling the temperature of the calibrator from 30°C to 40°C. In addition an attempt was made to thermally isolate the individual components within the calibrator and so measure the individual coefficients. The results of these measurements are shown in Table 1. The sensitivity of the calibrator to input a.c. voltage changes was undetectable being less than 1 ps per percentage voltage change.

Temperature Sensitivity of Phase Calibrator (Phase Delay)	
25 MHz low pass filter	+ 1.0 ± 5 ps/°C
Diode clipper	+ 10 ± 2 ps/°C
Wideband amplifier	- 3 ± 1 ps/°C*
Tunnel Diode	- 2 ± 1 ps/°C*
Overall sensitivity (measured separately)	6 ± 2 ps/°C

* A negative coefficient indicates that an increase in temperature decreases the phase delay through the device.

TABLE 1

$$\frac{\Delta V_P}{V_m} \simeq \text{fractional drift in } V_P$$

thus $\Delta t \simeq$ 20 ps/percentage drift

c) Variations in the delay through the filter and wide-band amplifier and diode attenuator.

5) Measurements of Calibrator Performance

a) Output power within a 360-kHz band was measured by comparing output with that of a noise tube. The level was found to be 60°K at 7850 MHz when coupled into the receiver through a 30 db coupler.

b) The stability of the calibrator was measured by observing the phase of the frequency rails from the calibrator (mixed down to 1 KHz) in the receiver video output. The overall sensitivity of the phase calibrator to temperature changes was measured by cycling the temperature of the calibrator from 30°C to 40°C. In addition an attempt was made to thermally isolate the individual components within the calibrator and so measure the individual coefficients. The results of these measurements are shown in Table 1. The sensitivity of the calibrator to input a.c. voltage changes was undetectable being less than 1 ps per percentage voltage change.

Temperature Sensitivity of Phase Calibrator (Phase Delay)

25 MHz low pass filter	+ 1.0 ± 5 ps/°C
Diode clipper	+ 10 ± 2 ps/°C
Wideband amplifier	- 3 ± 1 ps/°C*
Tunnel Diode	- 2 ± 1 ps/°C*
Overall sensitivity (measured separately)	6 ± 2 ps/°C

* A negative coefficient indicates that an increase in temperature decreases the phase delay through the device.

TABLE 1

Cable Measurement System

1) General Description

The delay through a cable changes with temperature (approx 1×10^{-4}°C) and flexure. Pressurized cables also change their electrical length with pressure. The phase-delay through a cable also varies in almost the same way as the group delay but with small differences owing to dispersion and multiple-reflection effects.

The cable measurement system was chosen from the following possible systems:

1. Phase detection of reflected sine wave using low-frequency modulation of reflected wave.
2. Phase detection of reflected sine wave using frequency translation of reflected wave.
3. Phase detection of the reflected wave using time multiplex.

Of the above systems, #1 appears to be the most free of systematic effects. Detection of the reflection at any frequency significantly different (more than a cable wavelength) from that transmitted results in errors due to cable dispersion and reflections while time multiplexing suffers from cross-modulation effects.

2) Theory

The transmitted signal $V_T(t)$ is reflected after modulation by $m(t)$ so that the signal received back at the transmitting end is

$$V_R(t) = m(t)\ \mathrm{Re}\ e^{i\omega_o t}\ e^{-2\phi i} \qquad \mathrm{Re} = \text{Real part of} \tag{5}$$

This signal is mixed with a version of the transmitted signal phase shifted by Φ and low-pass filtered to form

$$V_d(t) = m(t)\ \ \mathrm{Re}\ e^{-i2\phi}\ e^{i\Phi} \tag{6}$$

which is mixed with the modulation and low pass filtered again so that

$$V_o(t) = \langle m^2(t) \rangle \cos(2\phi - \Phi) \tag{7}$$

$V_o(t)$ is integrated and the loop closed on the phase shifter so that

$$\Phi = 2\phi + 2\pi (N \pm 1/4) \quad \text{where N is an integer constant.} \tag{8}$$

allowing the cable phase-delay ϕ to be measured from the measurement of Φ. A high resolution phase comparator has been developed for the measurement of Φ with picosecond precision. The comparator is described separately.

Phase servo noise analysis

The r.m.s. noise in the phase servo $\Phi_{r.m.s}$ is given by

$$\Phi_{r.m.s.} = \frac{1}{V} \left[\int \frac{N^2 d\omega}{|1 + j\omega/A\alpha V|^2} \right]^{1/2} \tag{9}$$

where N is the r.m.s. noise, V the r.m.s. signal voltage, referred to the input of the mixer. A is the overall voltage gain of the mixer, 5 KHz amplifier multiplier and integrator and α is the sensitivity of the phase shifter in radians per volt. Substituting the following values

$N \sim 10^{-9}$ volts/$\sqrt{\text{Hz}}$

$V \sim 10^{-3}$ volts

$A \sim 10^5$

$\alpha \sim 1$ radian/volt

we obtain and value of approximately 0.3 picoseconds.

Circuit Description

The cable measurement system consists of two units, one being located on the ground near the frequency standard and the other at the far end of the cable.

1) Ground Terminal

The ground terminal circuit is shown in Figure 4. The 5 MHz input signal is amplified in a +6 dB gain Buffer amplifier (circuit shown in Figure 5) and distributed to the cable, the phase shifter, the comparator reference and a digital divider. The reflected signal is mixed down with the buffered output of the phase shifter (see Figure 6 for the Buffer amplifier circuit) to an intermediate frequency of 5 KHz. The 5 KHz signal is then amplified and multiplied by the reference 5 KHz to provide the input to an integrator which closes the loop on the voltage controlled phase shifter.

The 5 MHz signal along with DC control signals and the 5 KHz modulation reference are all frequency multiplexed onto the one cable. Since the cable delay is less than a few microseconds it was decided to generate the modulation reference signal within the ground terminal to reduce the complexity of the "antenna" unit. The cable multiplexer circuit is shown in Figure 7. In addition it has a pulse input port which allows the return of a component of the tunnel diode pulse for scope viewing and counter synchronization.

2) "Antenna" Unit

The antenna unit circuit is shown in Figure 8. Most of the unit's circuitry is associated with the tunnel diode pulse generator whose circuit is shown in Figure 2B. The 5 MHz signal is divided to one 1 MHz in the pulse gate modulator (circuit shown in Figure 9) and used to drive the current controlled attenuator. A diode modulator is used to generate about 1% modulation of the reflection coefficient. The modulation is maintained at a fairly low level so that the 5 MHz driving the pulse generator is sufficiently isolated from the modulation to prevent the presence of significant 5 KHz sidebands in the calibration rails.

An analog DC control signal (0-10 volts) is decoded by conversion back to 2 bits of digital information. The most significant bit is used to switch on

and off the pulse generator and the least most significant bit is used to switch on and off a noise diode. The decoder circuit is shown in Figure 10.

Sources of systematic error in receiver phase and group delay calibration

There are many sources of systematic error not calibrated because the receiver response to the incoherent radio source signal differs from its response to the calibration pulses. For example spurious receiver responses (images and harmonic responses) are largely rejected in the correlation processing of radio source data from two receivers as the signals from different responses are uncorrelated. Table 2 summarizes the various effects on the receiver group delay.

Sources of Dispersion is the pulse generator output

The calibration pulse generator has some small amount of dispersion due to the inadequate attenuation of the unwanted pulses. 60 dB attenuation reduces the group delay ripple to less than 30 picoseconds. The ripple frequencies are subharmonics of 10 MHz so that averaging over several hundred MHz greatly reduces this defect. Multiple reflections between the pulse generator and the receiver can also cause frequency domain ripple a period that is the inverse of the reflection delay. This source of dispersion should be quite stable but will produce a delay difference between the 8.4 GHz and 2.3 GHz which will be less than 50 picoseconds provided multiple reflection is down 20 dB and the distance between the calibrator and the receiver is less than 1 meter.

Tests of the phase calibrator and cable measurement system

Tests of the phase calibrator have already been made and were presented in Haystack Technical Note 1975-1. Further tests are currently being conducted and will be separately documented.

Preliminary tests have been made of the cable measurement system. The temperature stability of both the ground and the antenna units have been separately measured and the results are shown in Figure 10. Measurements of the electrical length of a cable running from the Haystack control room up the antenna and back to the control room shows changes which are correlated with antenna motion. The cable appears to stretch rapidly with large antenna motion by an amount of up to 1 centimeter and then the cable relaxes slowly when the strain has been relieved by further antenna motion. A graph of these changes are shown in Figure 11. In addition tests have been made of the long term stability, accuracy and linearity.

System Specifications

1) Pulse Generator

Output rate	1 pulse/microsecond
Pulse width	<50 picoseconds
Pulse power (equivalent temperature including3dB power spit loss)	$20{,}000°K < T_{TD} < 50{,}000°K$ at 8.4 GHz $200{,}000°K < T_{TD} < 500{,}000°K$ at 2.3 GHz
Noise diode output (includes 13 dB loss)	$15{,}000°K < T_{ND} < 30{,}000°K$ at 8.4 GHz $50{,}000°K < T_{ND} < 100{,}000°K$ at 2.3 GHz
Stability of output with temperature	< 6 ps/°C
Dispersion ripple component (5 MHz ripple frequency)	< 50 ps
Dispersion $\tau_{8.4} - \tau_{2.3}$	< 50 ps

2) Cable measurement system

Resolution (set by comparator)	0.5 ps (one-way cable equivalent)
Stability - short term	$\pm$ 5 ps
- long term	$\pm$ 10 ps/hour

Absolute accuracy better than 100 ps

Linearity < 0.05%

Temperature coefficient of "Ground" unit: < 5 ps/°C

Temperature coefficient of "Antenna" unit: < 1 ps/°C

Parts List:

A) Buffer Amplifiers:

Resistors:	2 x 10Ω	1/8w
	1 x 10Ω	1/2w
	6 x 50Ω	1/8w
	5 x 100Ω	1/8w
	3 x 150Ω	1/4w
	1 x 150Ω	2w
	3 x 200Ω	1/4 w
Capacitors:	2 x 5 pF	
	12 x 0.05 µF	
	0.5µF	
	1.0µF	
Transistors:	4 x 2N5109	
IC's	2 x LH0033CG	

B) Cable Multiplex:

Capacitors:	2 x 25 pF
	2 x 200 pF
	2 x 0.01 Mylar
	2 x 0.3 Mylar
	2 x 0.1
Inductors:	2 x 0.1µH
	2 x 0.5 µH
	2 x 3.0 mH
Resistors:	2 x 1kΩ 1/8w

C) IF AMP/DETECTOR

Resistors: 1 x 68Ω 1/8w

2 x 100Ω 1/8w

1 x 200Ω 1/8w

6 x 1kΩ 1/8w

2 x 3kΩ 1/8w

1 x 6.8kΩ 1/8w

2 x 8kΩ 1/8w

2 x 100kΩ1/8w

1 x 150kΩ 1/8w

1 x 200 kΩ 1/8w

Capacitors: 2 x 4pF

1 x 12 pF

2 x 150pF

1 x 0.01 µF

2 x 0.03 µF

2 x 0.5 µF

2 x 1.5µF

1 x 10 µF 10v

1 x 22µF 15v

IC's 3 x LM308

1 x MC1495

1 x 74390

1 x 7490

1 x SN75140P

Transistors 2 x 2N3904

1 x 2N5109

D) Encoder

Resistors:	1 x 500Ω	
	1 x 1kΩ	
	1 x 9kΩ	
Capacitors	1 x 20pF	
	1 x 22µF	15v
IC	DAC371-8	

E) Modulator

Resistors:	1 x10Ω	
	1 x 47Ω	
	1 x 100Ω	
	1 x 5kΩ	
Capacitors:	2 x 0.01µF	
	1 x 20 µF	15v
Diodes:	4 x 1N4148. HP 5082-2835	

F) Pulse Gate Modulator

Resistors:	1 x 50Ω
	1 x 100Ω
	2 x 200Ω
	1 x 1kΩ
	2 x 4,7kΩ
Capacitors:	3 x 0.03 µF
	1 x 0.1 µF
IC's	1 x 7400
	1 x 7490
	1 x SN75140P
Transistors	3 x 2N918

G) Decoder

Resistors: 1 x 50Ω

4 x 100Ω

1 x 2kΩ

4 x 3kΩ

1 x 4kΩ 1/4w

IC's 1 x LM339N

1 x 7400

1 x 7406

Transistors 1 x 2N3904

H) Clipper: 1 x 50Ω

2 x 1N4121 or 1N5501 Diodes

1 Microbox

I) Tunnel diode Pulse Generator: 1 x 50Ω Microwave film resistor

1 x SMTD988 or TD273B GE Tunnel Diode

1 Microbox

Hardware:

1 Double width NIM module with connector

1 100μ A edge meter

1 10" x 4" x 4" aluminum box

1 DC Power supply Electrostatics Model 30 28V 1 AMP

~ 40 SMA connectors

3 Type N - 0.141" connectors

J) Commercial Parts

2 x O-H-30H Hybrids

2 x UTO-502 Avantek Amplifiers

1 x O-CDB-147 Mixer

1 x PSEM-45 Merrimac Phase Shifter

1 x NOR-1882-30 Noise Diode

1 x HP33124A Attenuator

1 x NARDA 4202B-10 Coupler

1 x NARDA 4303-2 Power Splitter

1 x UTO 502/503 Avantek Amplifier

1 x 10 dB Attenuator

Mechanical:

Figure 12 shows the "ground" unit which is contained in a double width NIM module. The antenna is built in an aluminum box complete with power supply as shown in Figure 13.

Systematic Effects on Group Delay

Defect	Effect on Calibrator	Effect on signal	Method of Elimination
Images or multiple receiver responses	$\Delta\tau \simeq \left(\frac{\alpha}{2\pi B}\right)$	small as image has different fringe rate	offset local oscillator or filter out image or both
Multiple reflections on antenna or within feed	none - unless calibrator radiates into feed from point on the antenna (however the near and far field multiple reflections may be different)	$\Delta\tau \simeq \left(\frac{\alpha}{2\pi B}\right)$	1) Model antenna - 2) use spectrometer - 3) distance measurements on antenna using optical or radio ranging devices
Differences in recording channels	depends on calibrator frequencies	$\Delta\tau \simeq \left(\frac{b\Delta t}{B}\right)$	commutation of channels
Receiver non-linearities	$\Delta \simeq \left(\frac{\beta}{2\pi B}\right)$	small	use wide dynamic range amplifiers with low intermodulation distortion

α = voltage rejection = $20 \log_{10}\alpha$ dB

B = effective bandwidth over which group delay is measured
≃ maximum frequency range covered

b = recording bandwidth

Δt = effective recording channel delay variations

β = intermodulation voltage rejection = $20 \log_{10}\beta$ dB

Table 2

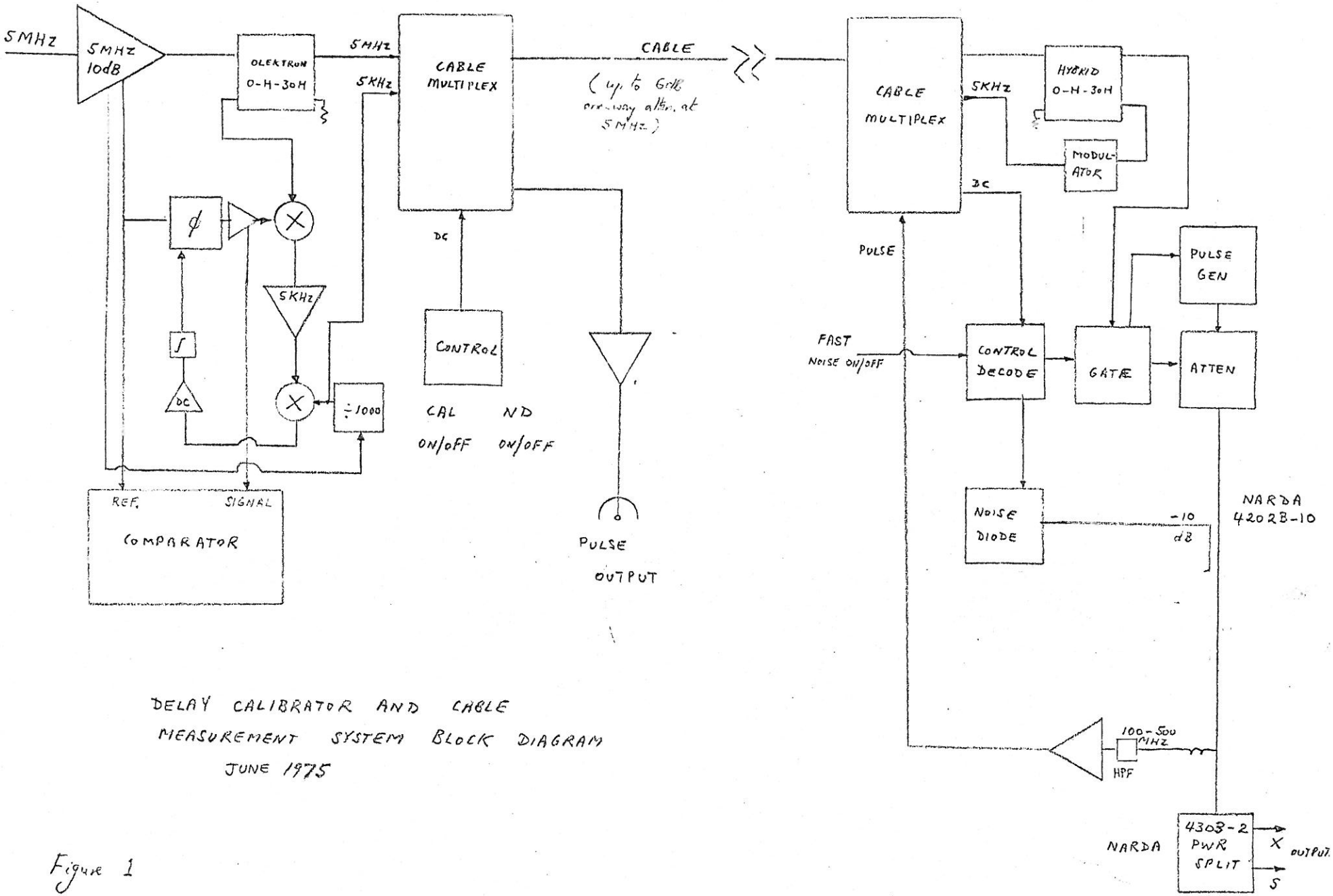

DELAY CALIBRATOR AND CABLE MEASUREMENT SYSTEM BLOCK DIAGRAM

JUNE 1975

Figure 1

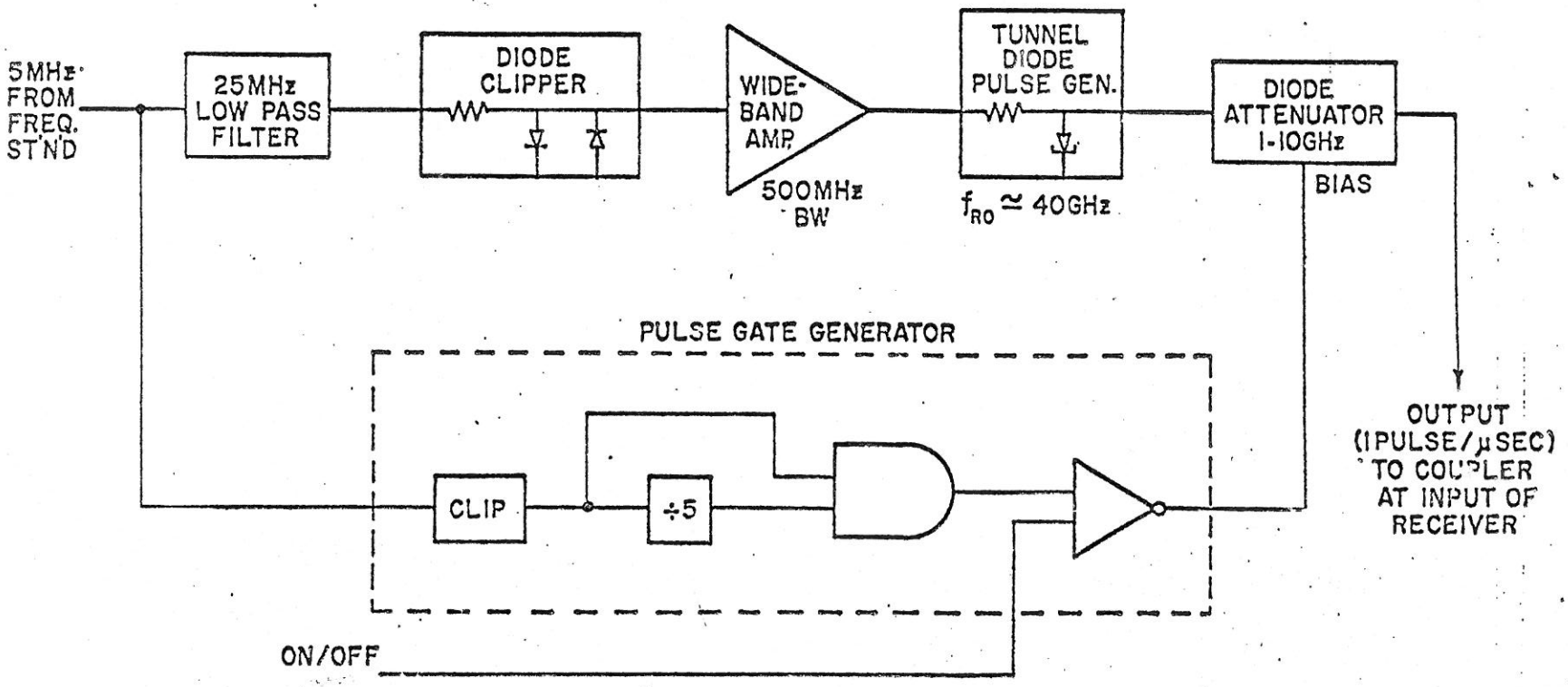
5MHz FROM FREQ. ST'ND
25MHz LOW PASS FILTER
DIODE CLIPPER
WIDE-BAND AMP
500MHz BW
TUNNEL DIODE PULSE GEN.
$f_{RO} \simeq 40$GHz
DIODE ATTENUATOR 1-10GHz
BIAS
PULSE GATE GENERATOR
CLIP
÷5
ON/OFF
OUTPUT (1PULSE/μSEC) TO COUPLER AT INPUT OF RECEIVER

FIG. 2A

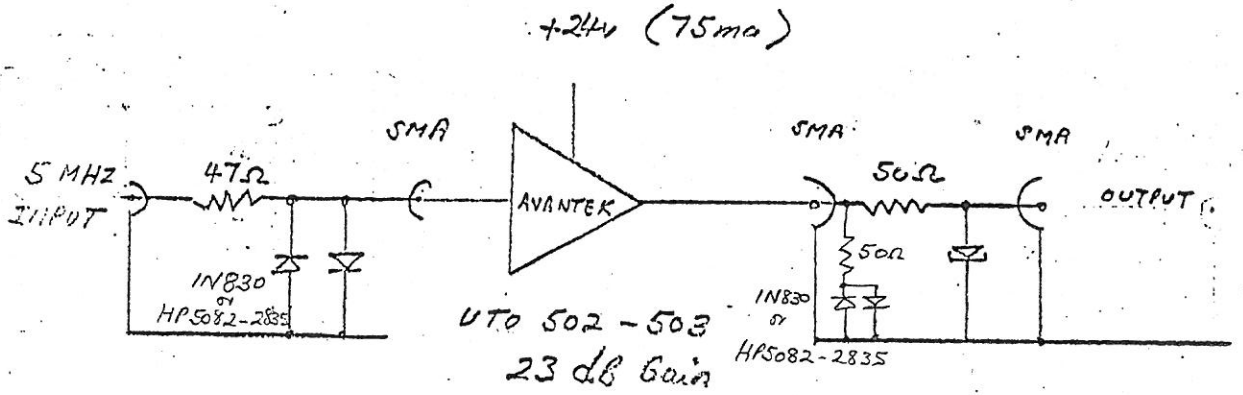

Note. Attenuator acts as HPF & DC block

VLB CALIBRATOR
PULSE GENERATOR

JAN 75

Fig. 2B

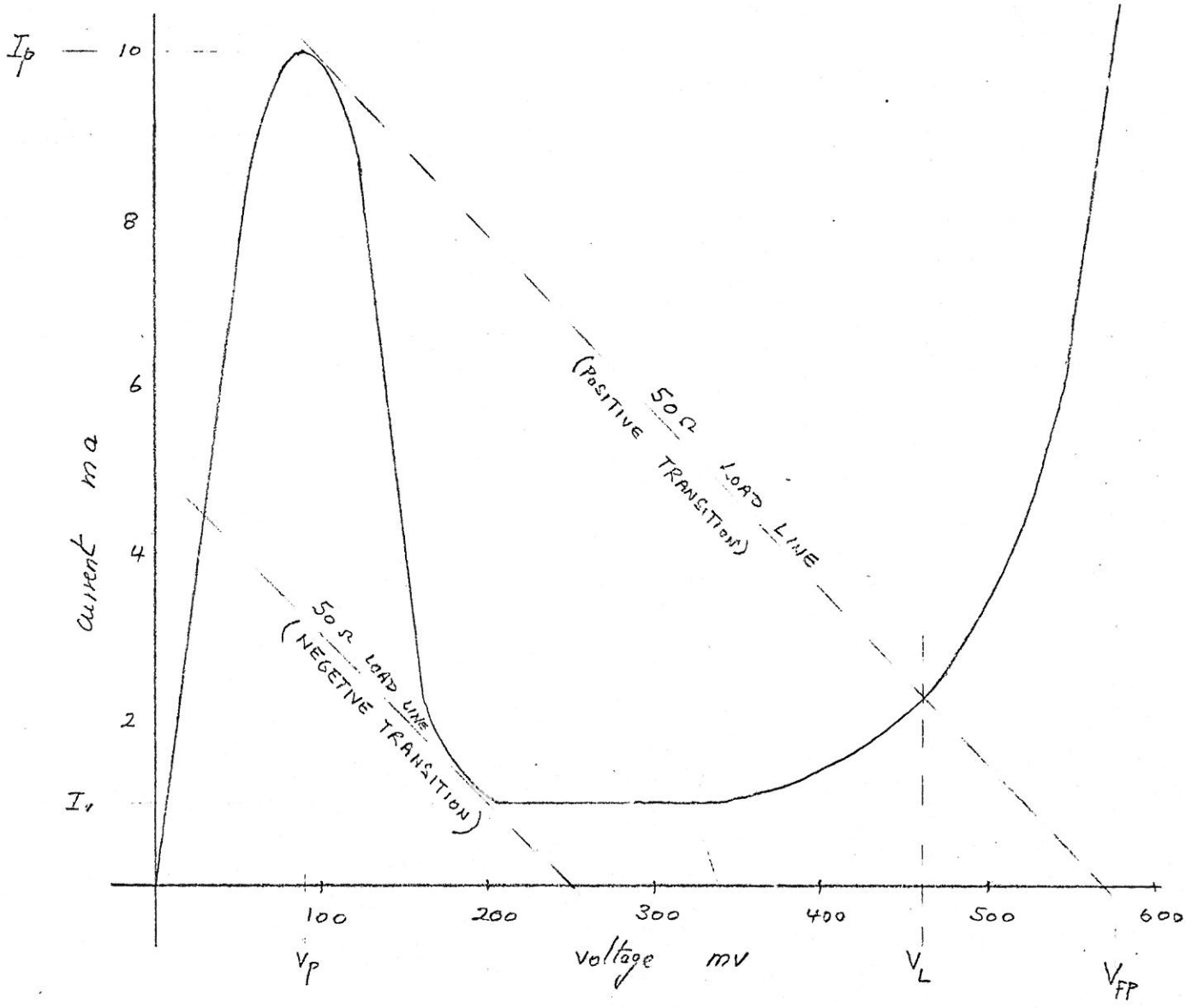

TUNNEL DIODE CHARACTERISTIC CURVE
(GE TD 273 B)

Figure 3

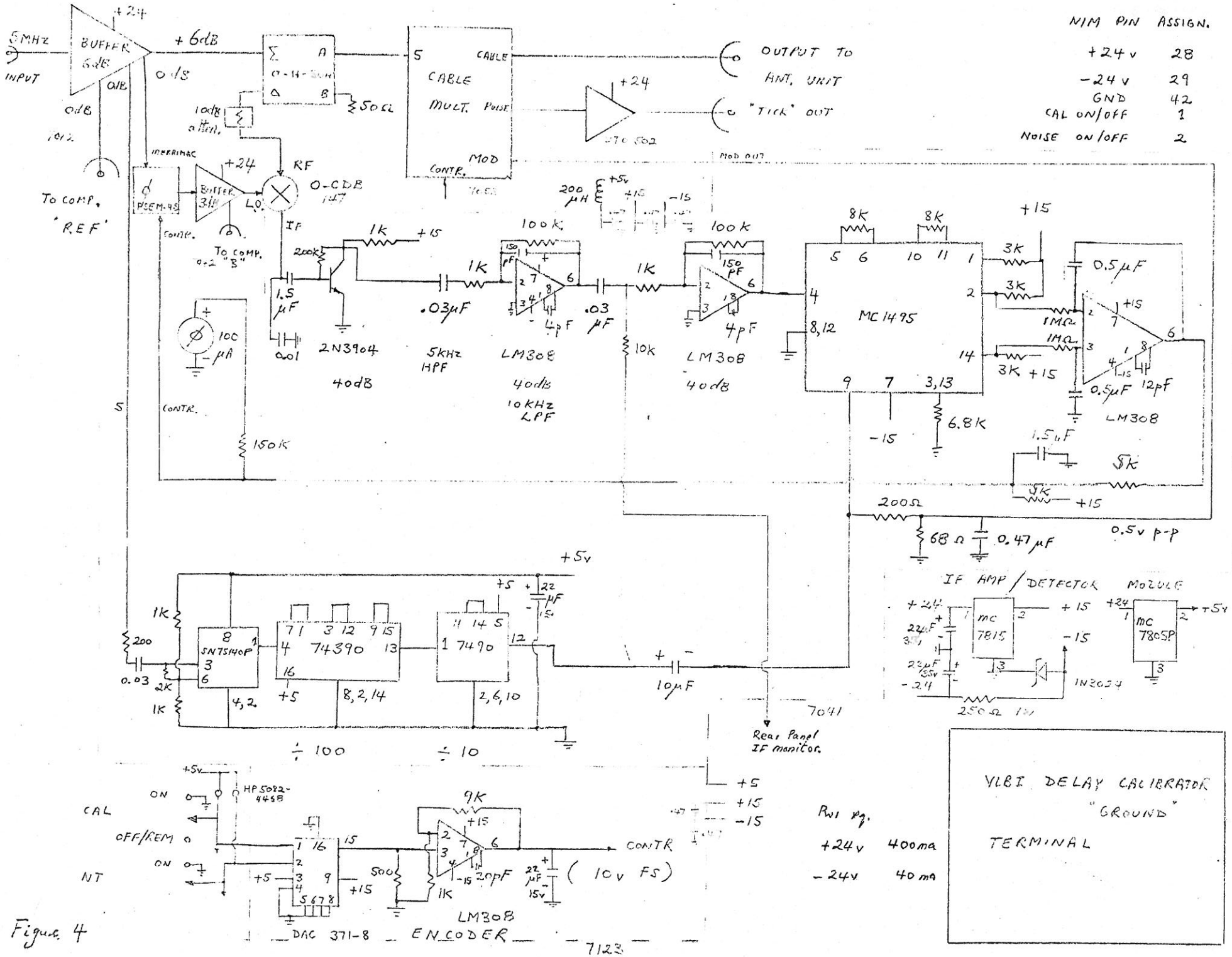
NIM PIN ASSIGN.
+24 v 28
-24 v 29
GND 42
CAL ON/OFF 1
NOISE ON/OFF 2
5MHz INPUT
BUFFER 6dB
+24
+6dB
0dB
0dB
10Ω
0 dB
50Ω
10dB atten.
CABLE MULT.
CABLE
MOD CONTR.
OUTPUT TO ANT. UNIT
"TICK" OUT
370 Ω
MERRIMAC PSEM-4S
BUFFER 31
LO
RF
IF
0-60dB
To COMP. 'REF'
To COMP. 0.2 "S"
CONTR.
100 μA
150K
1.5 μF
0.01
2N3904
40dB
1K
.03μF
5KHz HPF
200K
100K
150 pF
4pF
LM308
40dB
10KHz LPF
.03 μF
10K
8K
8K
MC 1495
8,12
14
9
7
3,13
-15
6.8K
3K
3K
3K +15
1MΩ
1MΩ
0.5μF
+15
12pF
LM308
1.5μF
5K
5K +15
200Ω
68Ω
0.47μF
0.5v p-p
200 μH
+5v
+15
-15
+5v
1K
200
0.03
2K
1K
8
SN75140P
1
4,2
74390
7 1 3 12 9 15
16
+5
8,2,14
7490
11 14 5
12
2,6,10
22 μF 15v
10μF
7041
Rear Panel IF monitor
÷ 100
÷ 10
IF AMP / DETECTOR MODULE
+24
22μF 35v
mc 7815
+15
-15
22μF 35v
-24
IN2054
250Ω 1w
mc 7805P
+5v
+5
+15
-15
Rwi Pg.
+24v 400ma
-24v 40 ma
CAL
ON
OFF/REM
ON
NT
HP 5082-4458
+5v
9K
+15
500
1K
20pF
22 μF 15v
(10v FS)
CONTR
LM308
DAC 371-8 ENCODER
7123
VLBI DELAY CALIBRATOR
"GROUND"
TERMINAL

Figure 4

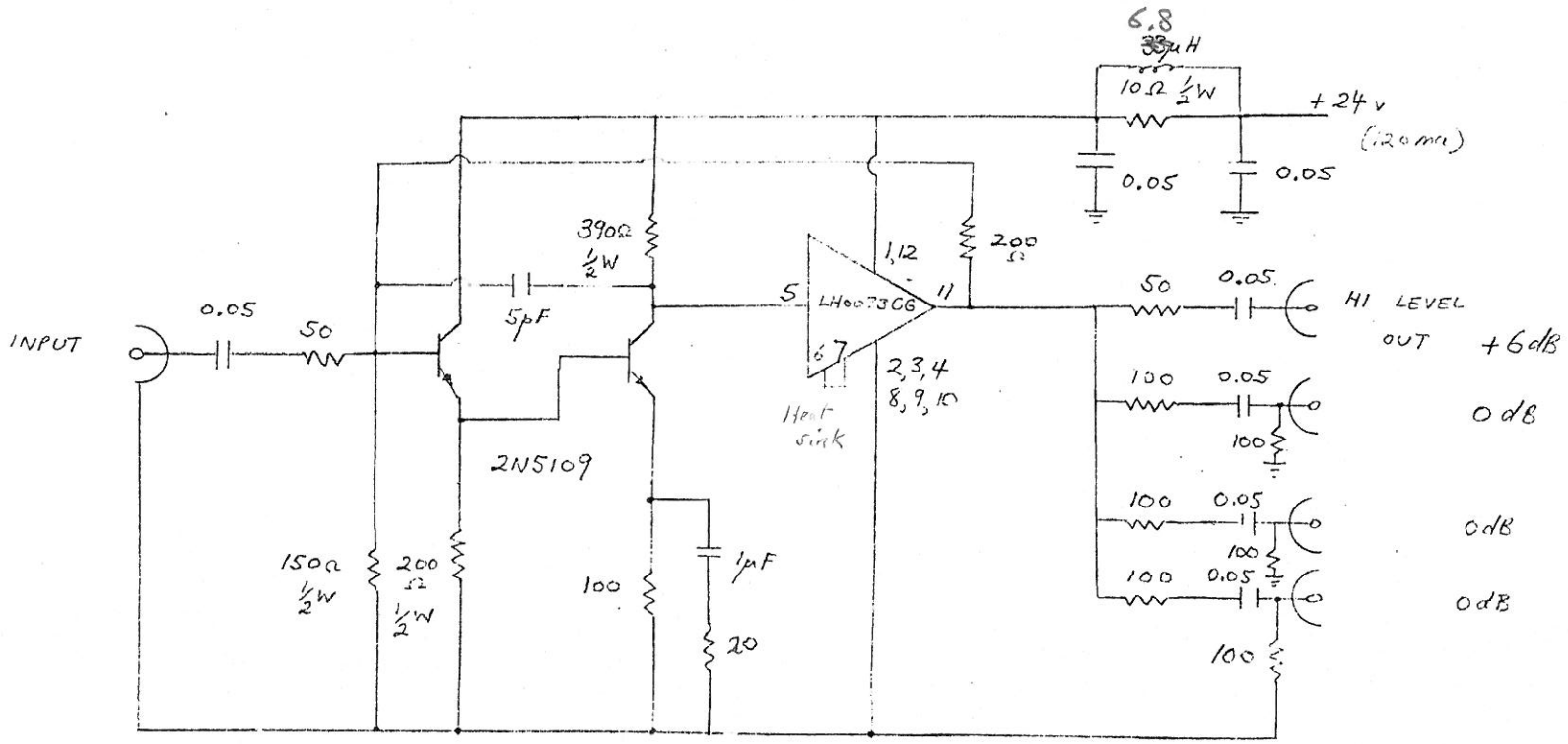

VLBI DELAY CALIBRATOR
+6dB BUFFER

Figure

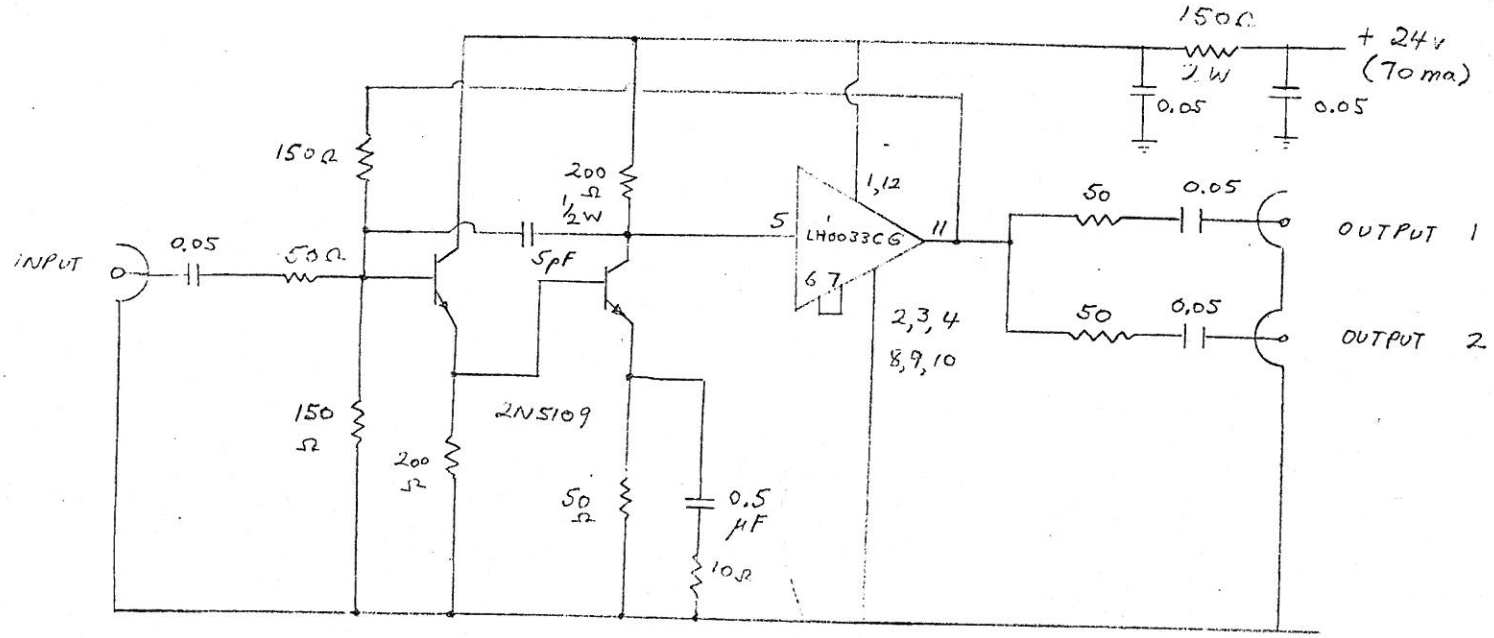

MEDPHR 7042

VLBI DELAY
CALIBRATOR
BUFFER
+30'B

Figure 6

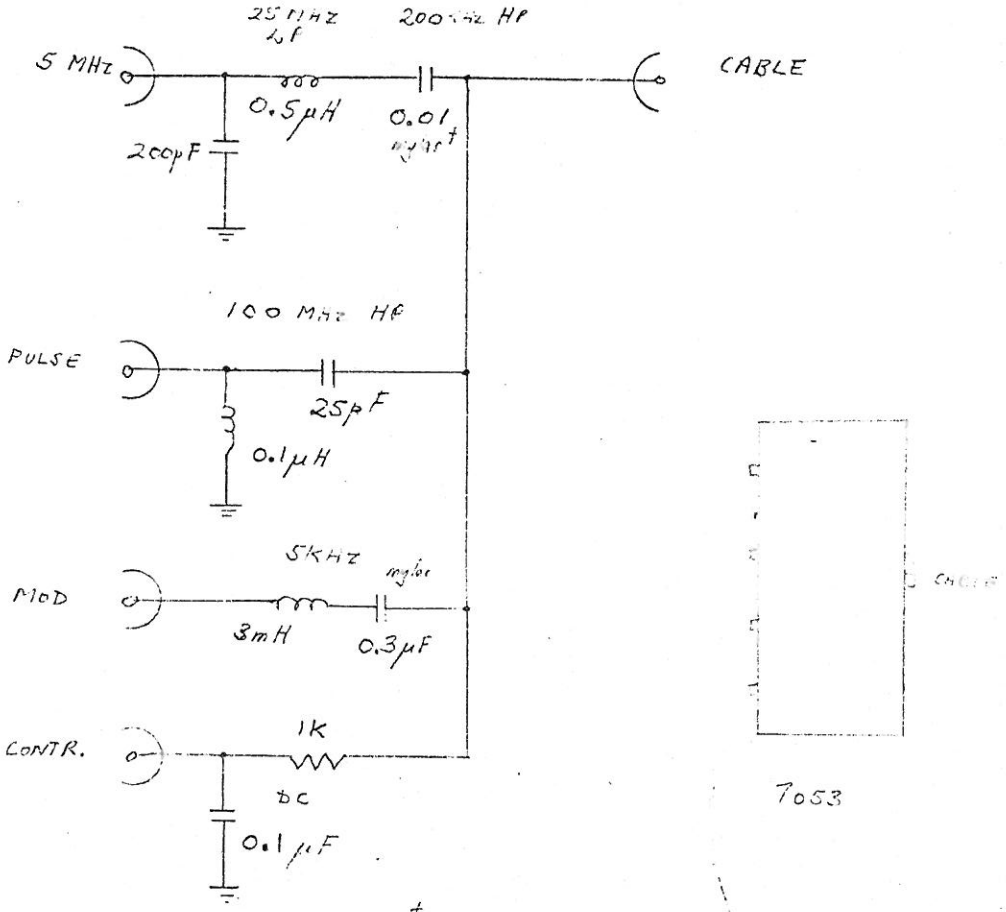

† To reduce 5kHz/5MHz intermodulation

VLBI DELAY CALIBRATOR

CABLE MULTIPLEX

Figure 1

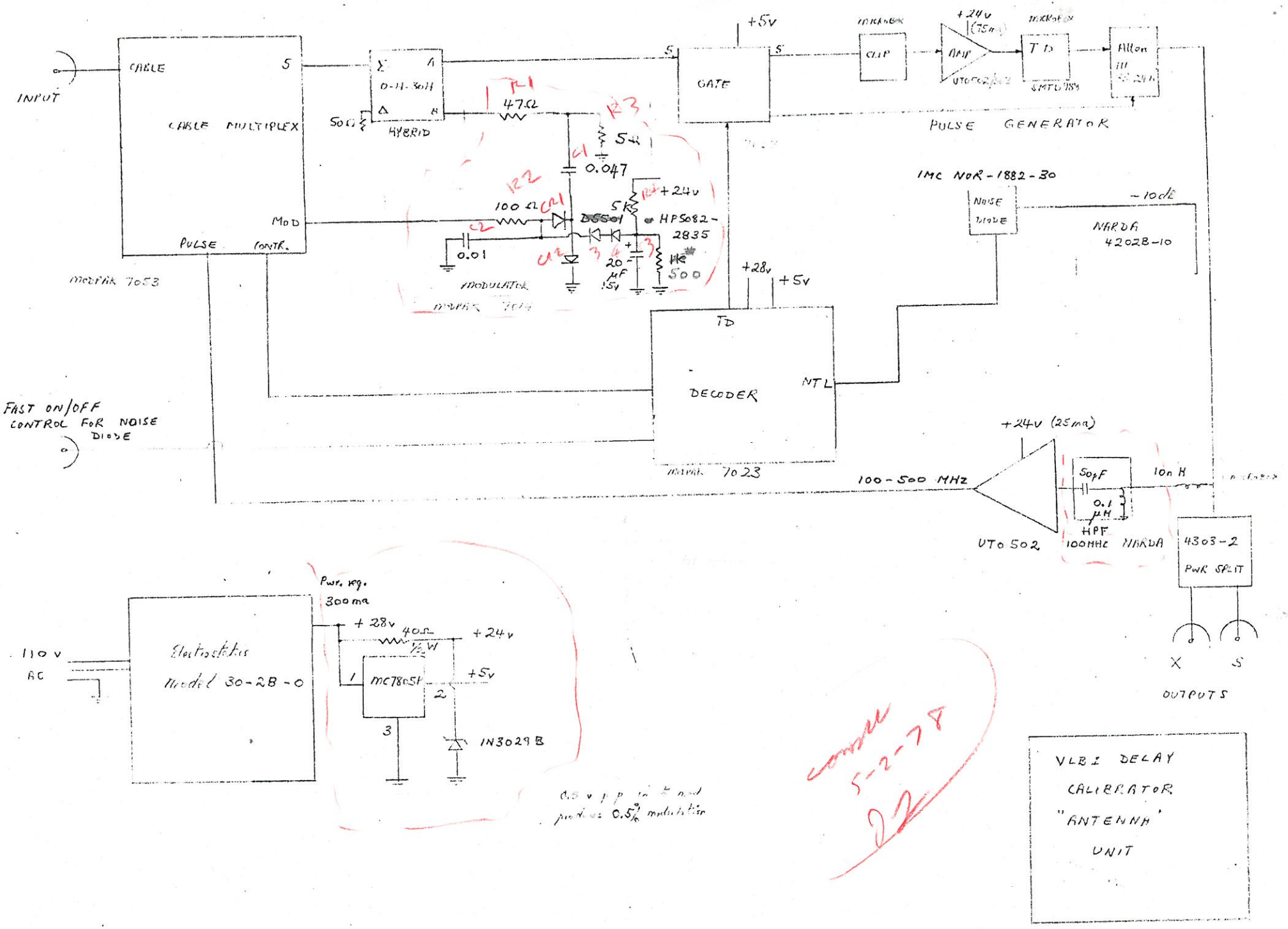
INPUT
CABLE
5
CABLE MULTIPLEX
MOD
PULSE CONTR.
MODEL 7053
Σ
Δ
A
B
0-11-30H
50Ω
HYBRID
R1
47Ω
R3
5Ω
C1
0.047
R2
100Ω
CR1
DSS01
R4
5K
+24v
HPS082-2835
C2
0.01
CR2
3
4
20 µF 15v
R5
500
MODULATOR
MODEL 7054
5
GATE
5
+5v
CLIP
+24v (75ma)
AMP
UTO 502
T D
SMTD 089
Allen
+28v
+5v
TD
DECODER
NTL
MODEL 7023
FAST ON/OFF CONTROL FOR NOISE DIODE
IMC NOR-1882-30
NOISE DIODE
-10dB
NARDA 42028-10
+24v (25ma)
100-500 MHz
UTO 502
50pF
10n H
0.1 µH
HPF 100MHz NARDA
4303-2
PWR SPLIT
X
S
OUTPUTS
110 v AC
Electrostatics
Model 30-2B-0
Pwr. Req. 300 ma
+28v
40Ω
½ W
+24v
1
MC7805P
2
+5v
3
IN3029B
0.5 v p-p in 1 mA
provides 0.5% modulation
VLBI DELAY CALIBRATOR "ANTENNA" UNIT
5-2-78
22

Figure 8

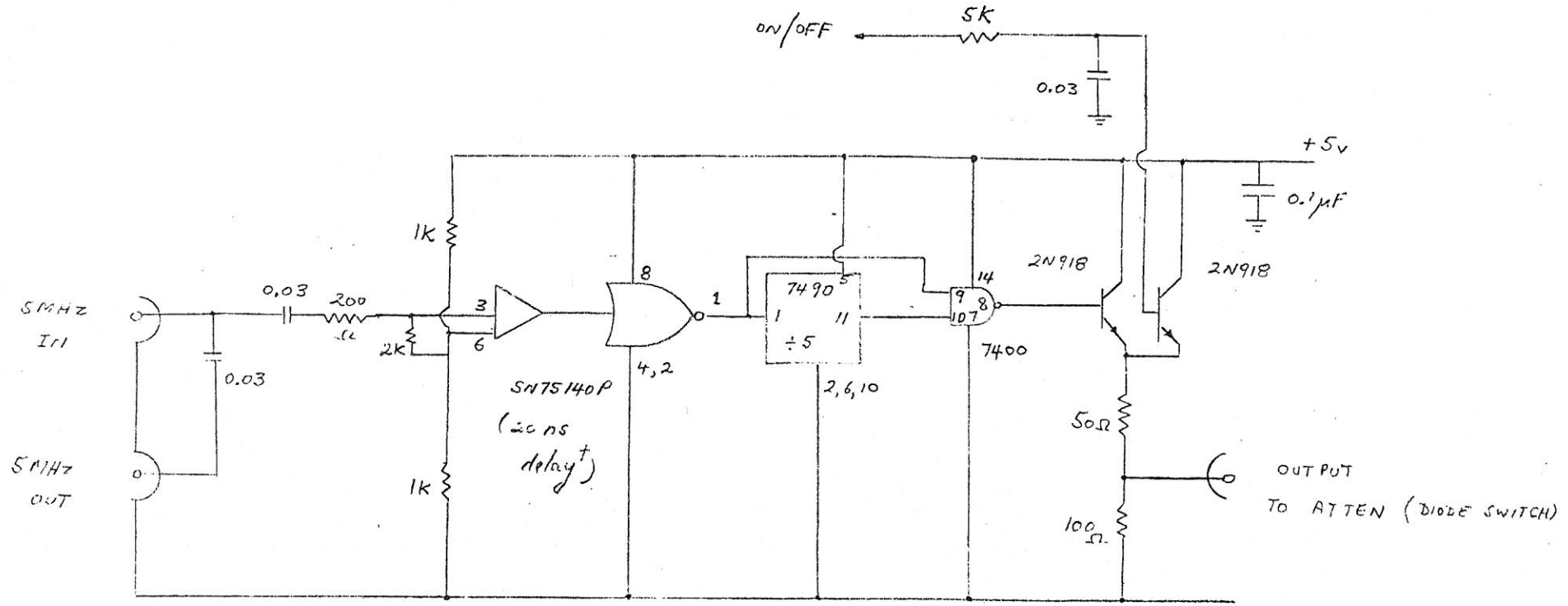

MODEL 7028-4

† Required to make switch operate with correct timing with respect to pulses emanating from tunnel diode.

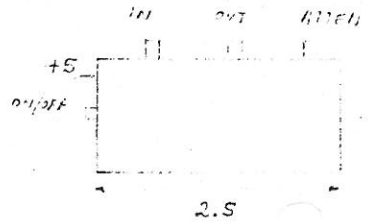

VLBI DELAY CALIBRATOR PULSE GATE MODULATOR

Figure 9

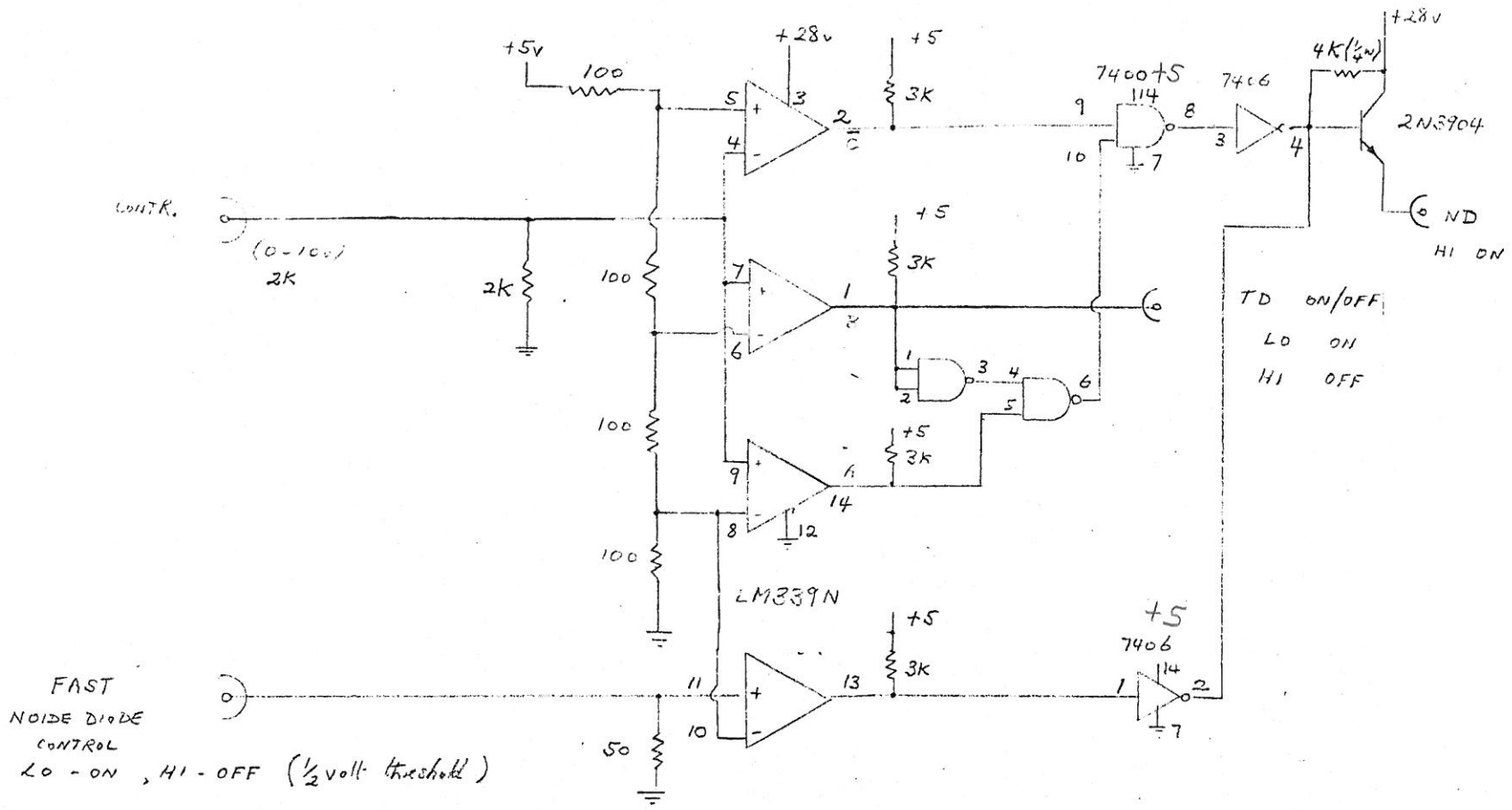

CAL NT	"ANALOG"	A	B	C	$\bar{C}$	TD	$A\bar{B}$	$A\bar{B}\bar{C}$	NT
ON ON	0 0	0	0	0	1	LO	1	1	HI
ON OFF	0 1	1	0	0	1	LO	0	0	LO
OFF ON	1 0	1	1	0	0	HI	1	1	HI
OFF OFF	1 1	1	1	1	0	HI	1	0	LO

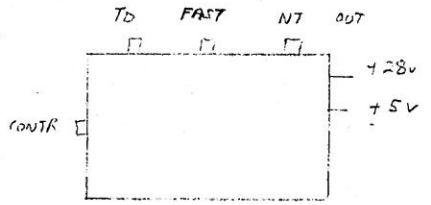

7023

VLBI DELAY CALIBRATOR

DECODER/DRIVER

Figure 10a

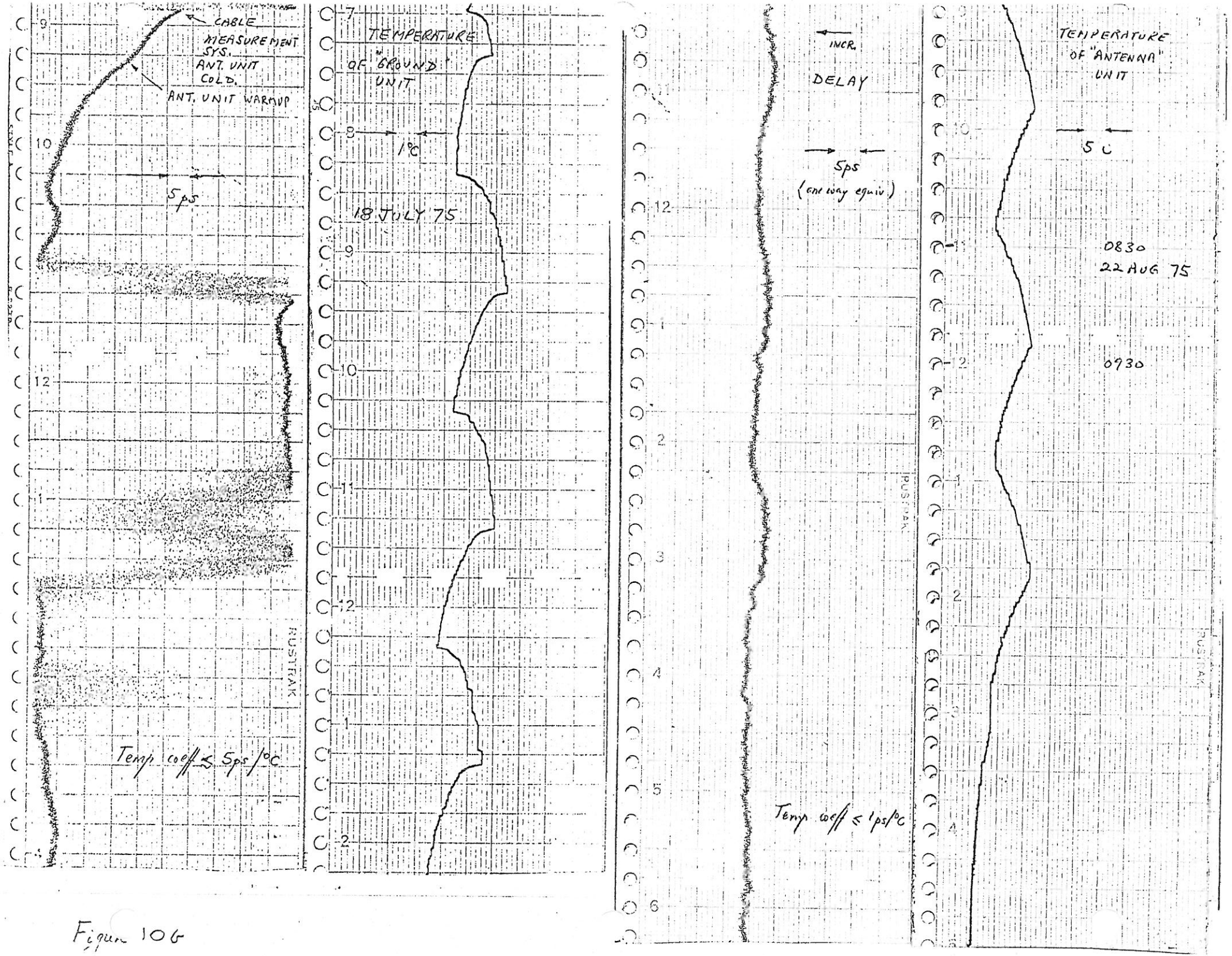
CABLE MEASUREMENT SYS. ANT. UNIT COLD.
ANT. UNIT WARMUP
5ps
Temp coeff ≤ 5ps/°C
TEMPERATURE OF "GROUND" UNIT
1°C
18 JULY 75
INCR. DELAY
5ps (one way equiv)
Temp coeff ≤ 1ps/°C
TEMPERATURE OF "ANTENNA" UNIT
5 C
0830 22 AUG 75
0930
RUSTRAK

Figure 106

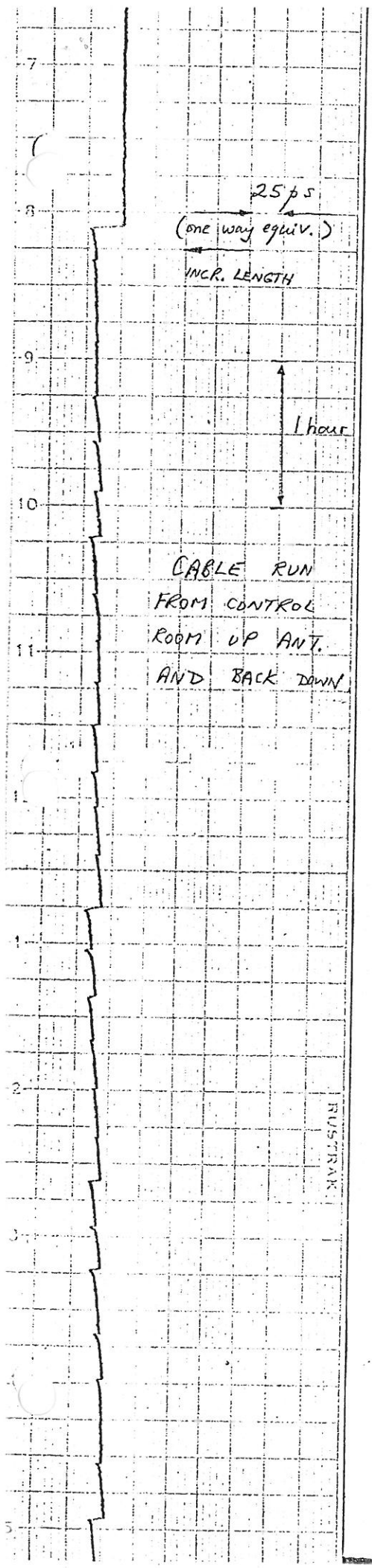

Figure 11. Stretching and relaxation of Haystack antenna cable.

VLBI DELAY
CALIBRATOR
5 MHZ INPUT
OFF/REM
PCAL
OFF/REM
NOISE
PHASE
REF SIGNAL
TO COMPARATOR
PULSE OUTPUT
CONTROL
VOLTAGE
30 V MAX

Figure 12

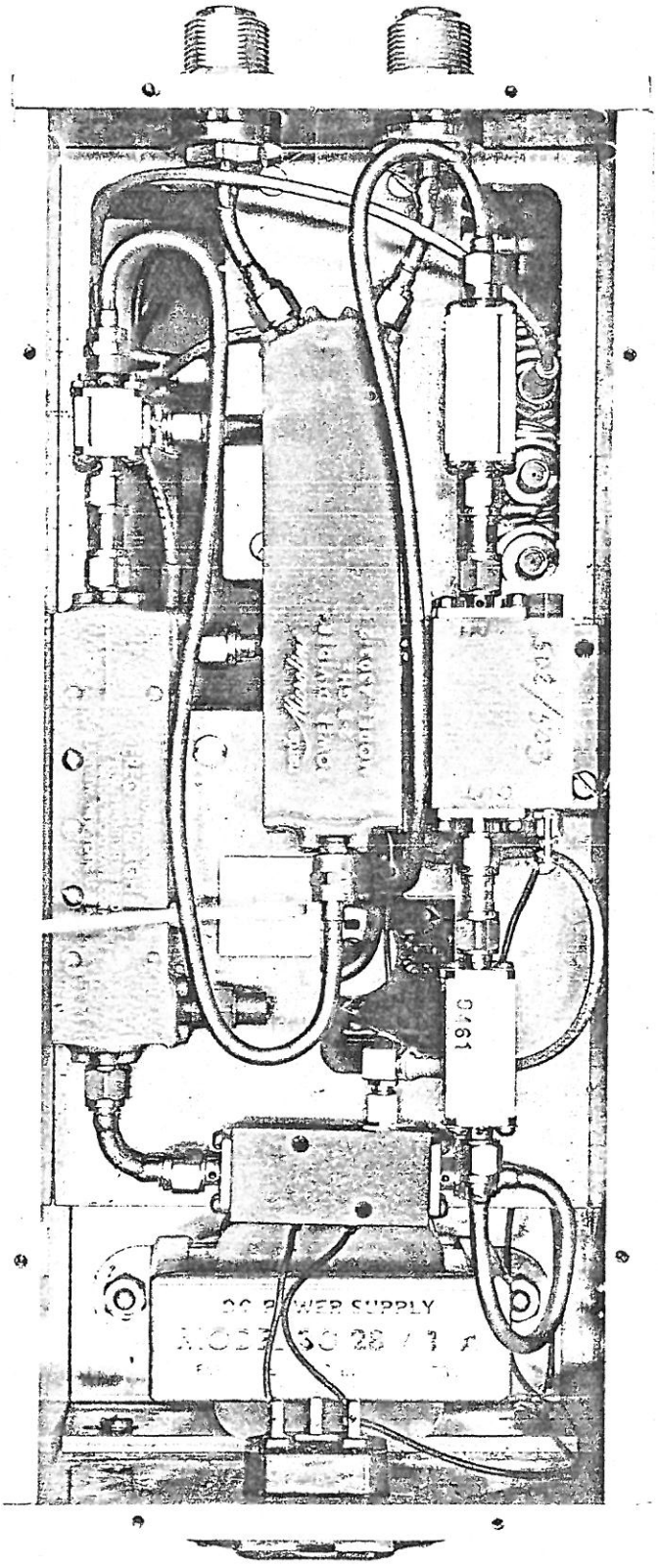

Figure 13